

CCUS: 4180432

Multi-Parameter Assessment of CO₂ Injectivity for Optimal Well Siting in Geological Carbon Storage.

Donna Christie Essel*¹, William Ampomah¹, Najmudeen Sibaweih², Dung Bui² 1. New Mexico Institute of Mining and Technology, 2. Petroleum Recovery Research Center.

Copyright 2025, Carbon Capture, Utilization, and Storage conference (CCUS) DOI 10.15530/ccus-2025-4180432

This paper was prepared for presentation at the Carbon Capture, Utilization, and Storage conference held in Houston, TX, 03-05 March.

The CCUS Technical Program Committee accepted this presentation on the basis of information contained in an abstract submitted by the author(s). The contents of this paper have not been reviewed by CCUS and CCUS does not warrant the accuracy, reliability, or timeliness of any information herein. All information is the responsibility of, and, is subject to corrections by the author(s). Any person or entity that relies on any information obtained from this paper does so at their own risk. The information herein does not necessarily reflect any position of CCUS. Any reproduction, distribution, or storage of any part of this paper by anyone other than the author without the written consent of CCUS is prohibited.

Abstract

Intensified climate mitigation efforts have highlighted Carbon Capture and Storage (CCS) as crucial for reducing CO₂ emissions. The efficacy of CO₂ storage in saline aquifers depends on the injectivity index. Although numerical simulations offer predictive insights, their high computational demands hinder quick basin-wide assessment. This study aims to address this challenge by developing an injectivity proxy model to expedite the identification of optimal injection sites. A CO₂ injection forecast set a base case for sensitivity analysis of injectivity parameters, including CO₂ viscosity, permeability-thickness product (kh), heterogeneity as Dykstra-Parson's coefficient (VDP), slope of the fractional flow curve (df/ds), injection rate, bottomhole pressure and permeability anisotropy. The dominant parameters were parameterized to generate the proxy for basin mapping. Sensitivity analysis revealed the most sensitive parameters governing CO₂ injectivity to be kh, VDP, CO₂ viscosity and df/ds. High kh coupled with VDP values above 0.52 resulted in larger plume extents and increased CO₂ saturation. Conversely, higher CO₂ viscosity produced lower CO₂ saturations and vice versa. Larger plume areas with less favorable CO₂ movement were observed for higher df/ds values. This was characterized by channeling of CO₂, leading to uneven displacement and flow patterns within the reservoir. The least sensitive parameters were injection rate and bottomhole pressure, both of which are contingent upon the aforementioned highly-sensitive parameters and permeability anisotropy. The San Juan basin CO₂ injectivity map generated from the proxy, delineates zones of high injectivity potential and that of lower injectivity prospects. The map provides a clear guidance on specific locations within the basin, optimum for placing CO₂ injection wells for effective climate action due to their capacity to safely inject and sequester substantial amounts of CO₂. This approach enables swift identification of promising well locations for injection, circumventing the need for time-consuming, comprehensive simulations. By streamlining site-selection processes, injectivity mapping accelerates preliminary evaluations, consequently enhancing the efficacy and cost-efficiency of CCS projects. This research not only advances the practical

implementation of CCS in the San Juan Basin but also provides a transferable framework for rapid, large-scale assessments of CO₂ injection in saline aquifers worldwide.

Introduction

Within Earth's dynamic biosphere, the carbon cycle plays a pivotal role, balancing the exchange of carbon dioxide (CO₂) between the planet's flora and fauna (Prajapati et al., 2023). This equilibrium has been markedly disrupted since the onset of the industrial era, leading to profound implications for global climate patterns, land use changes, diminished nutritional quality of certain crops, and biodiversity loss (Yang et al., 2024). The imperative to mitigate these trends has led to the advocacy for "net-zero" CO₂ emissions. Achieving this equilibrium necessitates integrating significant reductions in greenhouse gas emissions with enhanced carbon sequestration efforts (Barbhuiya et al., 2024). Among various geological formations, saline aquifers stand out for their potential to securely store vast amounts of CO₂ due to their large capacity, widespread occurrence and improved safety profile due to depth and isolation of these formations (Rasool et al., 2023). The feasibility and success of CO₂ sequestration projects in these formations hinges significantly on the injectivity index, a measure of the ease with which CO₂ is injected into the subsurface environment and the potential challenges that might arise during the injection process (Darkwah-Owusu et al., 2024). The injectivity index not only informs the design and operation of injection wells, but also plays a pivotal role in ensuring the long-term integrity of CCS projects (Mishra et al., 2017). Evaluation of CO₂ storage projects necessitates thorough site characterization, reservoir modeling, and development of monitoring strategies (Ma et al., 2024). During preliminary phases, the requisite depth of information for project evaluation may not be readily accessible to project developers; even when they are readily accessible, computational time and demands are a barrier. Furthermore, regulatory bodies tasked with scrutinizing detailed technical reports of projects may lean towards simpler analytical tools that provide a broad overview of the expected outcomes (Chen et al., 2022). Consequently, there is a need for the development of dependable screening models that can offer preliminary evaluations and aid in decision-making as addressed by this research. This model stands out for its minimal data requirements while maintaining a high level of accuracy compared to more complex simulation outcomes.

Methodology

This study focuses on the San Juan Basin in northwestern New Mexico, utilizing a 3D geological model covering 40x40 miles and extending 10,471 feet in depth. The model, subdivided into 806,850 grid cells and eight geological formations, highlights the Entrada Formation as its focal point. History matching was performed to refine the model before establishing a base case CO₂ injection scenario. A 30-year injection strategy was simulated using the SJB well to inject a 100% CO₂ stream with a surface rate limit of 18 MMcf/day and a bottomhole pressure of 4700 psi. Sensitivity analysis was conducted using Latin-hypercube sampling to evaluate the impact of key parameters, including permeability-thickness product (kh), permeability anisotropy, heterogeneity (V_{DP}), relative permeability, injection rate, bottomhole pressure (BHP) and CO₂ viscosity with the data shown in Table 1. While the well locations provide the kh, Equation 1 calculated the slope of the fractional flow curve, derived from Corey exponents for gas and water which represent the relative permeability relationship during the movement of CO₂ in the presence of brine. Several well locations were selected within the Entrada sandstone layer based on distinct hydraulic flow units, including a base case scenario at the existing SJB CO₂ injection well. Up to ten locations, summarized in Table 2, were analyzed to evaluate injectivity across the formation. For each site, the kh is deduced and V_{DP} computed with Equation 2. Relative permeability, modeled using Corey exponents, was assigned a range of 1 to 6 as per literature (Dria et al., 1993), with a base case value of 3 for both gas and water, reflecting laboratory-derived data. The viscosity of supercritical CO₂ was varied between 0.01 and 0.1 cP, consistent with typical supercritical CO₂ conditions (Prasad et al., 2023). Permeability anisotropy was parameterized within 0.1 to 0.6 (Clavaud et al., 2008). Operational

parameters, such as injection rates, were sampled from 10–25 MMSCF/day, while BHP was adjusted between 4,500 and 4,900 psi to maintain a fracture pressure gradient of 0.62 psi/ft, tailored to the basin.

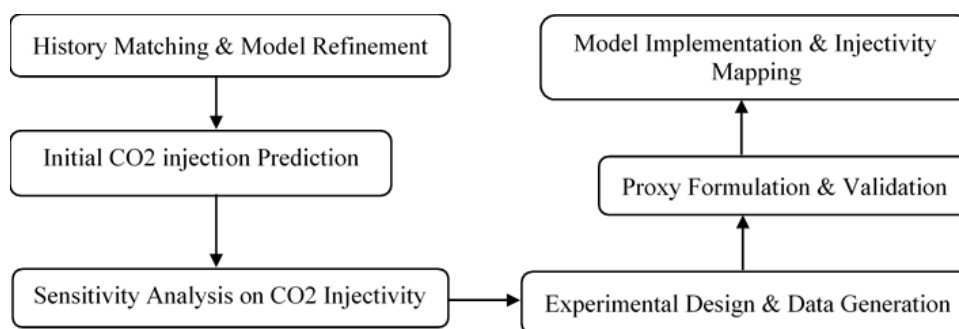


Figure 1. A summarized flowchart of the workflow designed for the study.

After identifying the most impactful parameters from sensitivity analysis displayed in Figure 3 – well location, df/ds , CO₂ viscosity, permeability anisotropy – 200 new numerical simulation runs were performed to obtain a dataset which was used in the proxy formulation. It adopts a machine learning approach based on Ridge regression to predict CO₂ injectivity due to its ability to handle multi-collinearity and stabilize solutions when dealing with highly correlated features, which are prevalent in geological datasets (Narayan et al., 2024). To prepare the data, the target is log-transformed to stabilize variance, and custom features are engineered to maintain consistency with the injectivity index's unit in MMcf/psi-day. The data is then split into training, testing, and blind test sets. To capture nonlinear relationships, polynomial transformations of degree 2 are applied, and features are standardized. A Ridge regression model is trained and optimized through cross-validation, selecting the best hyper-parameter to achieve high accuracy. The model's performance is evaluated on both test and blind datasets, using metrics such as R², mean squared error (MSE) and parity plots as seen in Figure 4 and Figure 5. The model is then implemented on the San Juan subsurface model to produce the injectivity map.

Results and Discussion

The study highlights how CO₂ plume dynamics are shaped by key reservoir properties fluid properties. Plumes were larger and more irregular in regions with high kh and V_{DP} , where CO₂ followed preferential flow paths, resulting in channeling and fingering. In contrast, low kh areas produced smaller, more stable plumes with uniform distribution, enhancing containment security. Steeper df/ds slopes led to aggressive brine displacement, increasing injectivity but causing irregular plumes, while gentler slopes resulted in stable CO₂ fronts. Similarly, low-viscosity CO₂ increased mobility, enabling rapid spread and uneven saturation, while high viscosity produced more controlled plumes, especially in homogeneous zones. Permeability anisotropy emerged as a moderate but impactful factor, with high anisotropy achieving lateral spread and low anisotropy balancing horizontal and vertical flow. Injection rate and BHP had minimal direct effects on plume dynamics as they are largely dictated by properties like kh , viscosity and anisotropy, thus suppressing the effect of the operational parameters. The Ridge regression model demonstrates a robust predictive capability for CO₂ injectivity, as evidenced by its equation and performance metrics. The model as displayed in Equation 4 emphasizes the dominant contribution of kh with the highest coefficient (0.0640), affirming its critical influence on injectivity while interaction terms underscore the complex interplay of key parameters in shaping injectivity dynamics. The model achieved near-perfect performance on the training and testing datasets, with R² scores of 0.999958 and 0.999922, respectively, and impressively low MSE values (8.22×10^{-7} for training and 1.15×10^{-6} for testing). These metrics indicate the model's ability to capture the underlying patterns in the data with accuracy. On the

blind test dataset, the model retains strong predictive capability, achieving an R^2 score of 0.875 and an MSE of 5.21×10^{-5} . These results confirm the model's ability to generalize well to unseen data, making it a reliable tool for practical applications in CO₂ injection planning and optimization.

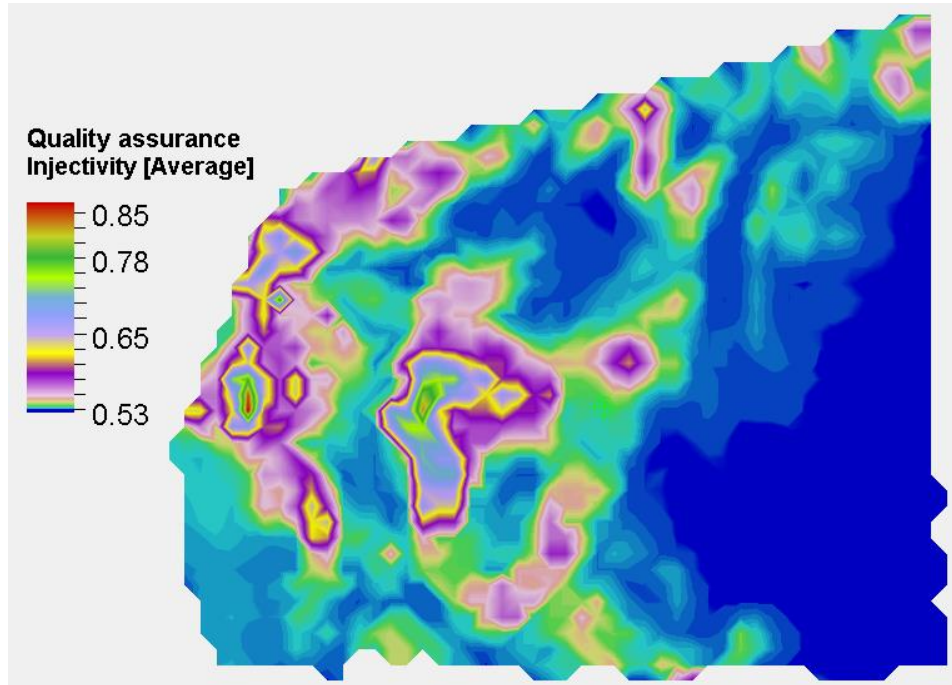


Figure 2. Average Injectivity map for the Entrada formation.

The average injectivity map in Figure 2 illustrates the spatial variability of CO₂ injectivity across the five layers of the Entrada formation, with values ranging from 0.53 to 0.85 MMcf/psi-day. Areas with high injectivity, represented by warmer colors, indicate zones of favorable reservoir properties such as higher kh values and moderate V_{DP} values. These regions are well-suited for CO₂ injection, as they facilitate efficient fluid flow and controlled plume development. Conversely, cooler-colored areas highlight regions of lower injectivity, which may correspond to tighter formations with increased variability in reservoir properties. These zones require tailored injection strategies, such as controlled injection rates or adjusted bottomhole pressures, to prevent issues like pressure buildup, uncontrolled plume spread or inefficient CO₂ storage. Overall, the injectivity map highlights the variability in reservoir quality within the Entrada formation. High-injectivity zones offer opportunities for efficient CO₂ injection, while lower-injectivity areas present challenges that must be addressed through tailored injection rates or pressure adjustments. This map enables the design of more efficient and secure injection strategies.

Conclusions

This study highlights the importance of reservoir and fluid properties in determining CO₂ injectivity, as well as the size and stability of CO₂ plumes. The Ridge regression model demonstrated exceptional predictive accuracy across training, testing, and blind datasets, confirming its reliability for injectivity estimation. Injectivity maps of the Entrada formation revealed substantial spatial variability, with high-injectivity zones offering opportunities for efficient injection and lower-injectivity areas requiring tailored strategies. These findings provide a practical framework for optimizing CO₂ storage in complex reservoirs.

References

- Prajapati, S.K., Kumar, V., Dayal, P., Gairola, A., Borate, R.B., and Srivastava, R. 2023. The Role of Carbon in Life's Blueprint and Carbon Cycle Understanding Earth's Essential Cycling System: Benefits and Harms to Our Planet. *AgriSustain-An International Journal* 01(1): 21-32. <https://doi.org/10.5281/zenodo.8385430>.
- Yang, Y., Tilman, D., Jin, Z., Smith, P., Barrett, C.B., Zhu, Y.G., Burney, J., D'Odorico, P., Fantke, P., Fargione, J., and Finlay, J.C. 2024. Climate change exacerbates the environmental impacts of agriculture. *Science* 385 (6713): eadn3747. <https://doi.org/10.1126/science.eadn3747>.
- Barbhuiya, S., Das, B.B., and Adak, D. 2024. Roadmap to a Net-Zero Carbon Cement Sector: Strategies, Innovations and Policy Imperatives. *Journal of Environmental Management* 359: 121052. <https://doi.org/10.1016/j.jenvman.2023.121052>.
- Rasool, M.H., Ahmad, M., and Ayoub, M. 2023. Selecting Geological Formations for CO₂ Storage: A Comparative Rating System. *Sustainability* 15 (6599). <https://doi.org/10.3390/su15086599>.
- Darkwah-Owusu, V., Md Yusof, M.A., Sokama-Neuyam, Y.A., Turkson, J.N., and Fjelde, I. 2024. A comprehensive review of remediation strategies for mitigating salt precipitation and enhancing CO₂ injectivity during CO₂ injection into saline aquifers. *Science of the Total Environment* 175232. <https://doi.org/10.1016/j.scitotenv.2024.175232>.
- Mishra, S., Ganesh, P. R., Kelley, M., and Gupta, N. 2017. Analyzing the Performance of Closed Reservoirs Following CO₂ Injection in CCUS Projects. *Energy Procedia* 114: 3465–3475. <https://doi.org/10.1016/j.egypro.2017.03.1477>.
- Ma, Z., Chen, B., Meng, M., and Pawar, R. 2024. Evaluation of CO₂ Storage Resources and Costs for the United States. Presented at the 17th International Conference on Greenhouse Gas Control Technologies (GHGT-17), Calgary, Canada, 20–24 October. <https://doi.org/10.2139/ssrn.5019817>.
- Chen, S., Liu, J., Zhang, Q., Teng, F., and McLellan, B.C. 2022. A Critical Review on Deployment Planning and Risk Analysis of Carbon Capture, Utilization, and Storage (CCUS) Toward Carbon Neutrality. *Renewable and Sustainable Energy Reviews* 167: 112537. <https://doi.org/10.1016/j.rser.2022.112537>.
- Dria, D. E., Pope, G. A., and Sepehrnoori, K. 1993. Three-Phase Gas/Oil/Brine Relative Permeabilities Measured Under CO₂ Flooding Conditions. *Software - Practice and Experience*. <https://api.semanticscholar.org/CorpusID:53927419>.
- Prasad, S.K., Sangwai, J.S., and Byun, H.S. 2023. A Review of the Supercritical CO₂ Fluid Applications for Improved Oil and Gas Production and Associated Carbon Storage. *Journal of CO₂ Utilization* 72: 102479. <https://doi.org/10.1016/j.jcou.2023.102479>.
- Clavaud, J.B., Alem, N., Trochet, P., and Adler, P.M. 2008. Permeability Anisotropy and Its Relations with Porous Medium Structure. *Journal of Geophysical Research: Solid Earth* 113 (1). <https://doi.org/10.1029/2007JB005004>.
- Narayan, S., Kumar, V., Mukherjee, B., Sahoo, S.D., and Pal, S.K. 2024. Machine Learning Assisted Reservoir Characterization for CO₂ Sequestration: A Case Study from the Penobscot Field, Canada Offshore. *Marine and Petroleum Geology* 169: 107054. <https://doi.org/10.1016/j.marpetgeo.2023.107054>.
- Mishra, S., & Ravi Ganesh, P. (2021). A screening model for predicting injection well pressure buildup and plume extent in CO₂ geologic storage projects. *International Journal of Greenhouse Gas Control*, 106(January), 103261. <https://doi.org/10.1016/j.ijggc.2021.103261>.

Appendix

Table 1. Summary of input data for sensitivity analysis.

Parameter	Unit	Base	Minimum	Maximum
Well Location	-	1	1	10
Corey Gas	-	3	1	6
Corey Water	-	3	1	6
Viscosity	cP	0.05	0.01	0.1
Anisotropy	-	0.1	0.1	0.6
Injection Rate	MMscf/day	18	10	25
BHP	psi	4700	4500	4900

Table 2. Permeability-thickness product and heterogeneity at sampled well locations for location sensitivity analysis.

X	Y	kh	V _{DP}
85	72	1813.21	0.53
27	143	1536.04	0.374
80	144	86.15	0.45
132	142	14.09	0.52
24	108	440.88	0.55
66	107	297.16	0.61
133	109	5.84	0.351
135	69	17.96	0.45
78	79	6300.63	0.58
124	30	290.05	0.57

Equation 1. Fractional flow of gas (CO₂) to formation brine (Mishra and Ravi Ganesh, 2021).

$$f_g = \frac{\frac{k_{rg}}{\mu_g}}{\frac{k_{rg}}{\mu_g} + \frac{k_{rw}}{\mu_w}}$$

Equation 2. Permeability heterogeneity calculation for the log-normal permeability distribution (Mishra and Ravi Ganesh, 2021).

$$V_{DP} = \frac{k_{50} - k_{84.1}}{k_{84.1}}$$

Equation 3. Calculating CO₂ Injectivity (Mishra and Ravi Ganesh, 2021).

$$Injectivity = \frac{Injection\ rate}{Bottomhole\ pressure - Reservoir\ pressure}$$

The Ridge Regression Algorithm for CO2 Injectivity Prediction

Input:

- Training set, $S = \{(X_1, y_1), (X_2, y_2), \dots, (X_m, y_m)\}$
- Polynomial degree, $d = 2$
- Ridge regularization hyper-parameter, α
- Log-transformed target, $y_{\log} = \log(1+y)$

Process:

- Constructing custom features
 - CustomFeature1 = X_4/X_1 (kh/ μ_{CO2})
 - CustomFeature2 = X_2 (df/ds)
 - CustomFeature3 = X_3 (Anisotropy)
 - CustomFeature5 = X_5 (V_{DP})
- Standardization, $\hat{X} = (X-\mu)/\sigma$
- Initialize Ridge Regression Model

$$\hat{y}_{\log} = \underset{\beta_0, \beta_1, \dots, \beta_p}{\operatorname{argmin}} \sum_{i=1}^n \left(y_{\log,i} - \beta_0 - \sum_{j=1}^p \beta_j \hat{X}_j \right)^2 + \alpha \sum_{j=1}^p \beta_j^2$$

- Compute predicted log-values, $\hat{y}_{\text{test, log}} = \text{Model}(\hat{X}_{\text{test}})$
- Reverse the log transformation, $\hat{y}_{\text{test}} = \exp(\hat{y}_{\text{test, log}}) - 1$
- Compute evaluation metrics

$$MSE = \frac{1}{n} \sum_{i=1}^n (y_{\text{test},i} - \hat{y}_{\text{test},i})^2$$

$$R^2 = 1 - \frac{\sum (y_{\text{test}} - \hat{y}_{\text{test}})^2}{\sum (y_{\text{test}} - \bar{y})^2}$$

- Blind Test Evaluation and metrics calculation
- Visualizations
- Ridge Regression Equation Output

$$Y = \exp \left(\beta_0 + \sum_{j=1}^p \beta_j \text{Feature}_j \right) - 1$$

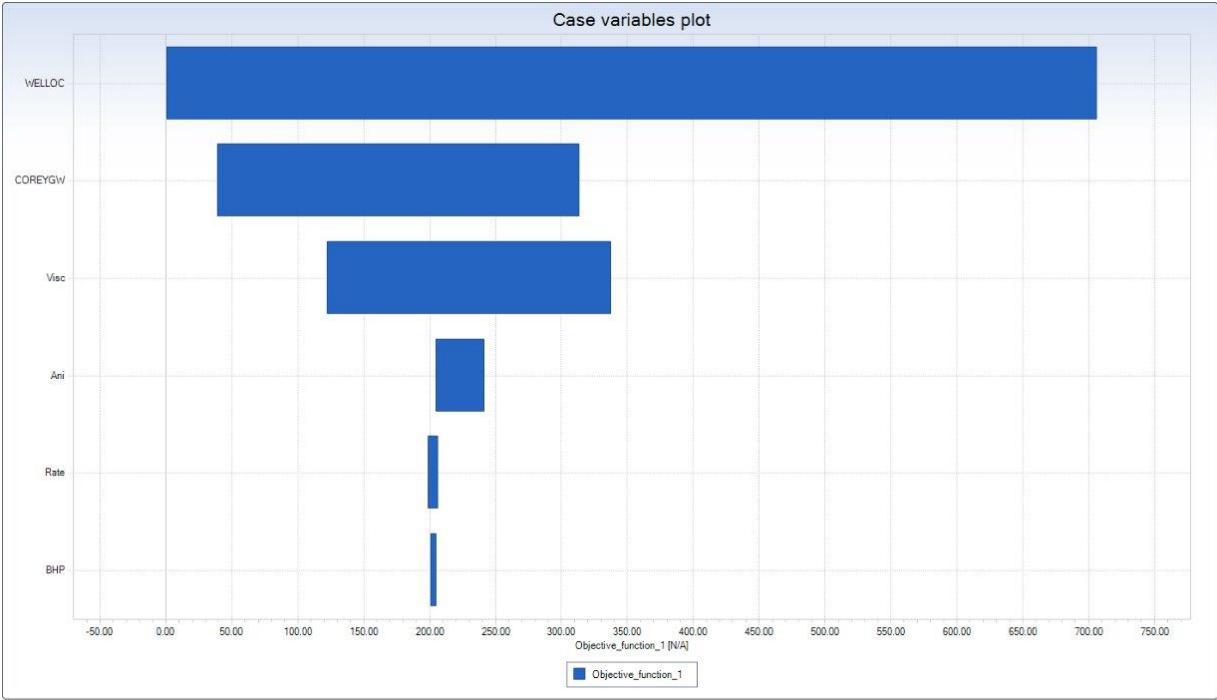


Figure 3. Relative impact of each variable on CO2 injectivity.

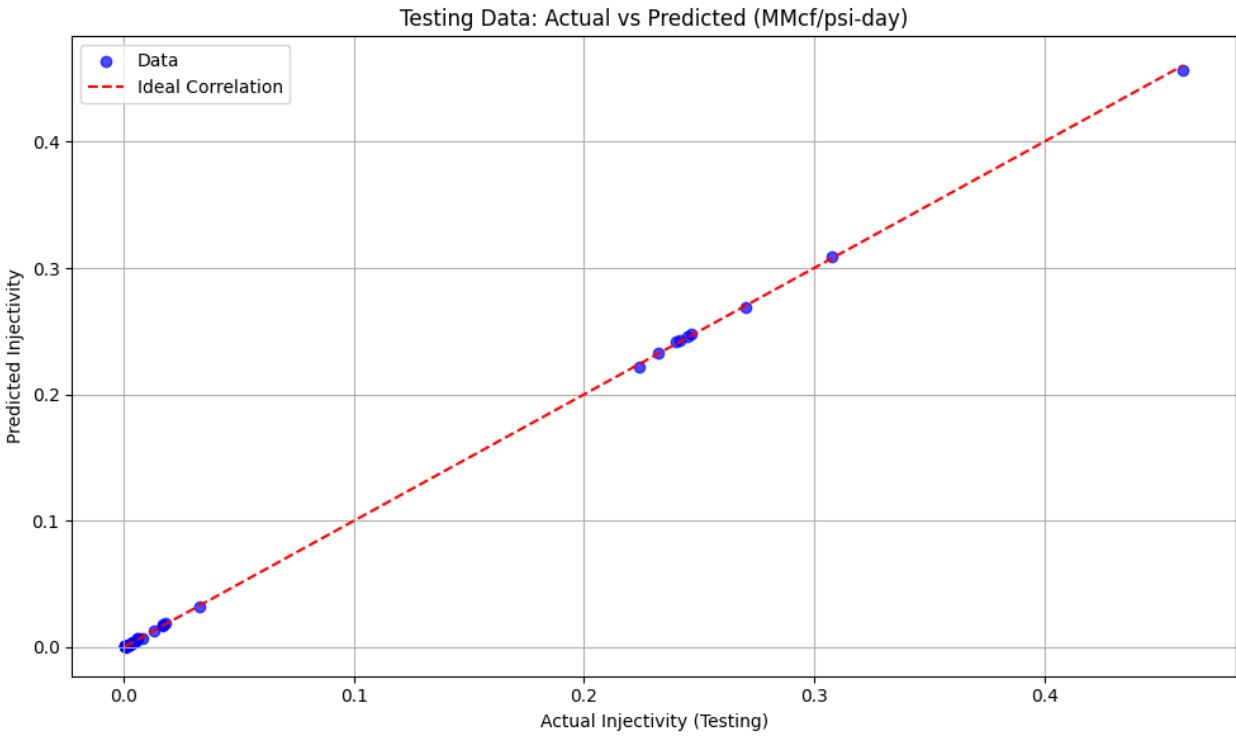


Figure 4. Actual vs. predicted test result for general data pool.

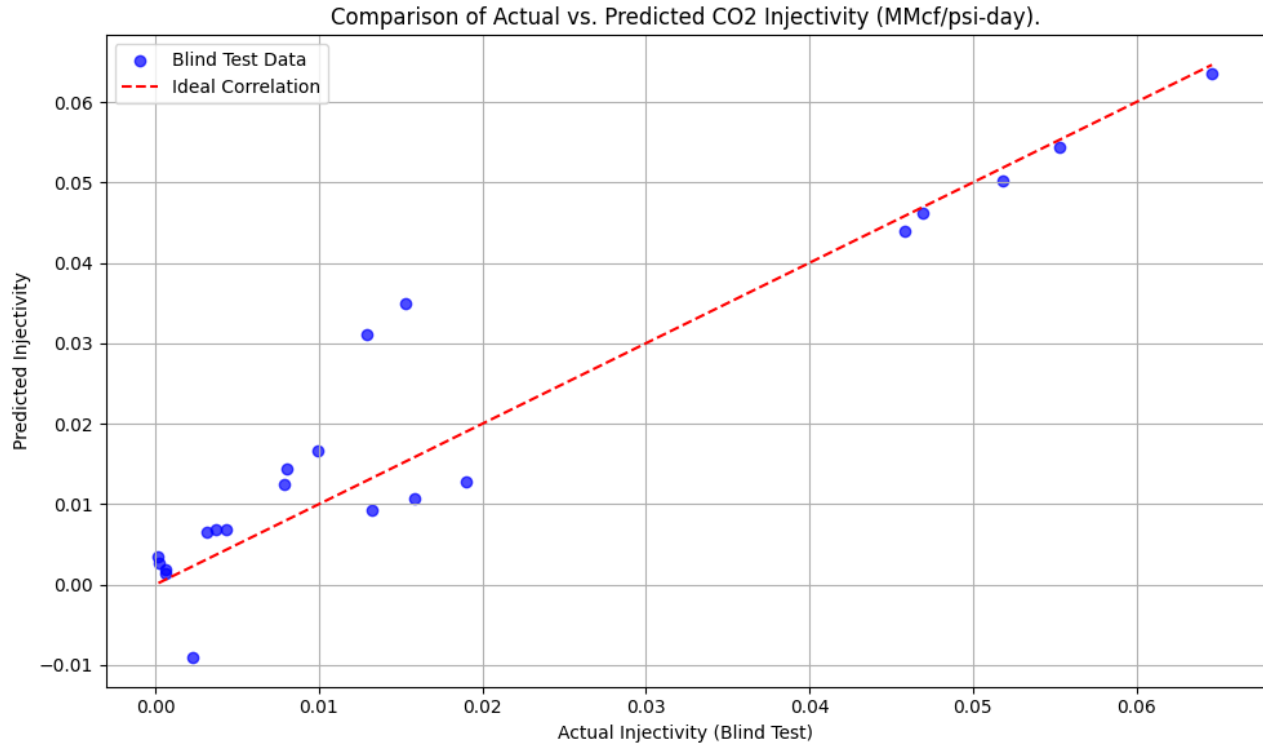


Figure 5. Parity plot of actual vs. predicted for blind data set.

Equation 4. Ridge Model of CO2 Injectivity.

$$\begin{aligned}
 Y = \exp & \left[0.0814 + \left(0.064 \frac{X_4}{X_1} \right) + (0.0345X_2) + (0.0583X_3) + (0.0038X_5) + \left(0.0612 \frac{X_4^2}{X_1^2} \right) + \left(-0.0216 \frac{X_4X_2}{X_1} \right) \right. \\
 & + \left(-0.0833 \frac{X_4X_3}{X_1} \right) + \left(0.0737 \frac{X_4X_5}{X_1} \right) + (0.0085X_2^2) + (-0.0506X_2X_3) + (0.005X_2X_5) \\
 & \left. + (0.0163X_3^2) + (-0.0193X_3X_5) + (0.0034X_5^2) \right] - 1
 \end{aligned}$$

Where

Y = CO2 Injectivity, MMcf/psi-day

X₁ = CO2 Viscosity, psi-day

X₂ = Slope of fractional flow curve, df/ds

X₃ = Permeability Anisotropy

X₄ = Permeability-thickness product (kh), cf

X₅ = Heterogeneity, V_{DP}